

# Susceptibility of Some Electronic Equipment to HPEM Threats

Daniel Nitsch, *Senior Member, IEEE*, Michael Camp, *Student Member, IEEE*, Frank Sabath, *Member, IEEE*, Jan-Luiken ter Haseborg, *Fellow, IEEE*, and Heyno Garbe, *Senior Member, IEEE*

**Abstract**—In this paper, an overview of the susceptibility of a large number of different electronic devices like computer networks, computer systems, microprocessor boards, microcontrollers, and other basic integrated circuits (ICs) to different threats like electromagnetic pulse (EMP), ultrawideband (UWB), and high-power microwave pulses (HPM) is given. The presented data will include a comparison of the HPM and UWB susceptibility of some devices and a deeper look into the destruction effects in ICs. Therefore, the ICs were opened and the destruction effects were investigated. A norm based approach to describe the threat of different pulses to electronic devices gives a theoretical explanation for the measured susceptibility data.

**Index Terms**—Electromagnetic effects, electromagnetic pulse, electronic equipment, EMP, susceptibility, UWB.

## I. INTRODUCTION

COMMUNICATION, data processing, sensors, and similar electronic devices are vital parts of the modern technical environment. Damage or failures in those devices could lead to technical or financial disasters as well as injuries or the loss of life. The significant progress of the high-power electromagnetic (HPEM) source and antenna technologies and the easy access to simple HPEM systems entail the need to determine the susceptibility of electronic equipment to those threats.

The assessment of different circuit and pulse parameters on the upset and destruction effects are important to develop models for the susceptibility behavior and protection elements.

## II. THREAT PARAMETERS

In our investigations three different HPEM pulse threats were applied to the equipment under test (EUT): double exponential pulses, bipolar pulses, and microwave pulses.

Nuclear electromagnetic pulses (NEMP) and unipolar ultrawide-band pulses (UWB) generally have a double exponential pulse shape with the characteristic parameters rise time ( $t_r$ ), the

Manuscript received July 16, 2003; revised April 13, 2004.

D. Nitsch and F. Sabath are with Federal Armed Forces Scientific Institute for Protective Technologies and NBC-Protection (WIS), Munster, Germany (e-mail: DanielNitsch@bwb.org). <<Author: Is the definition for "WIS" correct? Also, please provide postal code, thank you>>

M. Camp is with the Institute of Electrical Engineering and Measurement Science, University of Hannover, Hannover, Germany. <<Author: Please provide postal code, thank you>>

J. L. ter Haseborg is with the Department of Electrical Engineering and Electromagnetic Engineering, University of Hamburg-Harburg, Hamburg, Germany <<Author: Please provide postal code, thank you>>

H. Garbe is with the Department of Electrical Engineering and Information Technology, University of Hannover, Hannover, Germany <<Author: Please provide postal code, thank you>>

Digital Object Identifier 10.1109/TEMC.2004.831842

TABLE I  
TYPICAL PARAMETERS FOR NEMP, UWB, AND HPM

Pulse Shape	Parameter 1	Parameter 2	Parameter 3
NEMP	$t_r$ few ns	$t_{fwhm}$ 20 – 400 ns	$E_{max}$ 50 kV/m
Unipolar UWB	$t_r$ 90 – 250 ps	$t_{fwhm}$ few ns	$E_{max}$ 1 – 100 kV/m <sup>1</sup>
Bipolar UWB	$t_r$ 50 – 250 ps	$t_{pp}$ 100 – 500 ps	$E_{max}$ 1 – 100 kV/m <sup>1</sup>
HPM	$f_c$ 500 MHz – 5 GHz	$t_d$ 50 – 500 ns	$E_{max}^*$ 1 – 100 kV/m <sup>1</sup>

<sup>1</sup>Field Strength is depending on the distance between the source and the target.

\* Peak value of the electrical field

maximum electric field strength ( $E_{max}$ ) and the full width half max time ( $t_{fwhm}$ ). Radiated pulses usually have a bipolar pulse shape that is characterized by the rise and fall time ( $t_r$  and  $t_f$ ) the time between maximum and minimum field strength ( $t_{pp}$ ) and the maximum electric field strength ( $E_{max}$ ). High-power microwave pulses (HPM) are characterized by the maximum electric field strength ( $E_{max}$ ), their duration ( $t_d$ ), and their center frequency ( $f_c$ ). Table I shows some typical parameters for the different HPEM threats.

## III. DEFINITIONS

To describe the different failure effects, two quantities were defined. The breakdown failure rate (BFR) was defined as the number of breakdowns of a system, divided by the number of pulses applied to it (see Fig. 1). A breakdown means no physical damage is done to the system. After a reset (self-, external-, or power reset) the system goes back into function. The breakdown threshold (BT) specifies the value of the electrical field strength, at which the BFR gets 5% of the maximum value. The breakdown bandwidth (BB) is defined as the span of the electrical field strength, in which the BFR changes from 5% to 95% of the maximum. The DFR of the device under test has been defined as the number of destructions divided by the number of pulses applied to the system. Destruction is defined as a physical damage of the system so that the system will not recover without a hardware repair.

As shown in [1], the breakdown and destruction efficiency of

$$\|V(j\omega)\|_{f,p}^{(f_1, f_2)} = \left\{ \int_{f_1}^{f_2} |V(j\omega)|^p d\omega \right\}^{\frac{1}{p}} \quad (1)$$

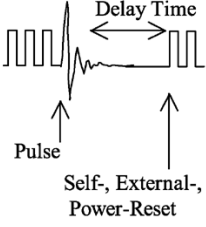
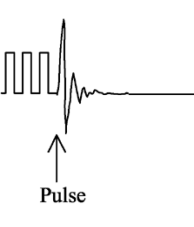
<u>B</u> reakdown	<u>D</u> estruction
 <p>Delay Time</p> <p>Pulse</p> <p>Self-, External-, Power-Reset</p>	 <p>Pulse</p>
<u>B</u> reakdown <u>F</u> ailure <u>R</u> ate	<u>D</u> estruction <u>F</u> ailure <u>R</u> ate
$BFR = \frac{\text{No. of Breakdowns}}{\text{No. of Pulses}}$	$DFR = \frac{\text{No. of Destructions}}{\text{No. of Pulses}}$

Fig. 1. Definition of the BFR and DFR.

pulses can be calculated with their field strength spectrum  $V(j\omega)$  and the frequency range  $[f_1, f_2]$  in which the EUT is coupling in a resonant behavior. This description is based on frequency limited norms [2] which are defined in (1).

With those norms it is possible to describe the threat parameters of a given wide-band pulse. The most interesting efficiencies are the energy- and amplitude efficiency  $\eta_E$  and  $\eta_A$ , which describe how much of the energy and the amplitude

$$\eta_E = \frac{\|V(j\omega)\|_{f,2}^{(f_1,f_2)}}{\|V(j\omega)\|_{f,2}} \quad \eta_A = \frac{\|V(j\omega)\|_{f,1}^{(f_1,f_2)}}{\|V(j\omega)\|_{f,\infty}} \quad (2)$$

of a given pulse is coupling into the EUT.

To calculate the real threat potential of a given pulse to a EUT, described by his resonant coupling range  $[f_1, f_2]$ , one has

$$\rho_A = \|V(j\omega)\|_1^{f_1,f_2} \quad \rho_E = \|V(j\omega)\|_2^{f_1,f_2} \quad (3)$$

to evaluate the average spectral amplitude  $\rho_A$  and energy density  $\rho_E$ :

#### IV. GENERAL MEASUREMENT SETUP

All susceptibility data was taken by applying an electro-magnetic field to the EUT in a TEM structure. Exemplary, we will describe the two mostly used TEM waveguides (see Figs. 2 and 3) and the setup of the different EUT. The open area waveguide is a NEMP test simulator with a maximum height of about 23 m described in [3]. The laboratory waveguide [4] is an open waveguide inside a shielded room enclosed by absorber walls. The absorbers at the end of the waveguide were placed on interchangeable wooden walls. The position of the septum can be adjusted via nylon threads. The measurements of the electromagnetic properties were carried out with a time-domain reflectometer (TDR) as well as electric and magnetic ground plane and free field probes.

The different EUT were placed in the TEM structure as shown in Fig. 4. During the test procedure, different EUT signals as well as the field pulse were monitored with a real time scope (bandwidth: 6 GHz sampling rate: 20 GSample/s).



Fig. 2. Open area TEM waveguide at the WIS, Munster, Germany.

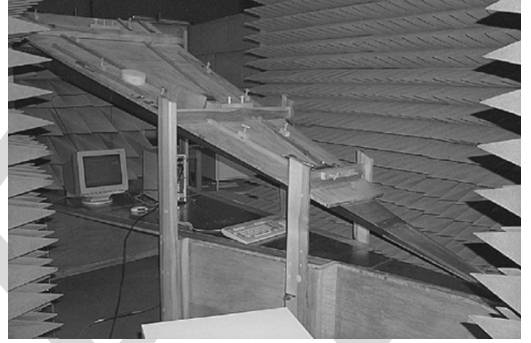


Fig. 3. Laboratory TEM waveguide at the WIS, Munster, Germany.

#### V. MEASUREMENT RESULTS

In this section, a short extract of the most interesting results of the susceptibility investigations is given. Different electronic devices like logic elements, microcontrollers, PC systems, and PC networks were tested.

##### A. Logic Devices

During the investigations, ten different semiconductor technologies (six TTL, four CMOS families) have been tested (see Table II) concerning the susceptibility to electromagnetic pulse (EMP) and Ultrawide-band (UWB) pulses <<Author: Please define "TLL" thank you>>. NANDs, inverter, generic array logic devices, and shift registers were chosen to observe the influence of the technology on the destruction effects.

To apply the different pulses to the EUT, modular setup has been realized (Fig. 5). Ten separate channels were built with a combination of differently printed circuit boards. The circuit boards were combined with ribbon cables to realize different coupling lengths at the input and output pins of the devices under test.

The power supply was made with ten different accumulators. DIP switches were implemented in the power supply unit to adjust arbitrary bit patterns at the input pins <<Author: Please define "DIP" thank you>>. LEDs and resistors were used as loads to observe the operating states of the devices. As a first result, it can be noticed that CMOS-devices first are affected by reversible breakdowns that are fixed by switching the power off and on. At much higher field amplitudes destructions occur. This effect can be explained by a parasitic thyristor (latch up effect) as a result of the vicinity of complementary n- and p-channel transistors in CMOS devices described in [5].

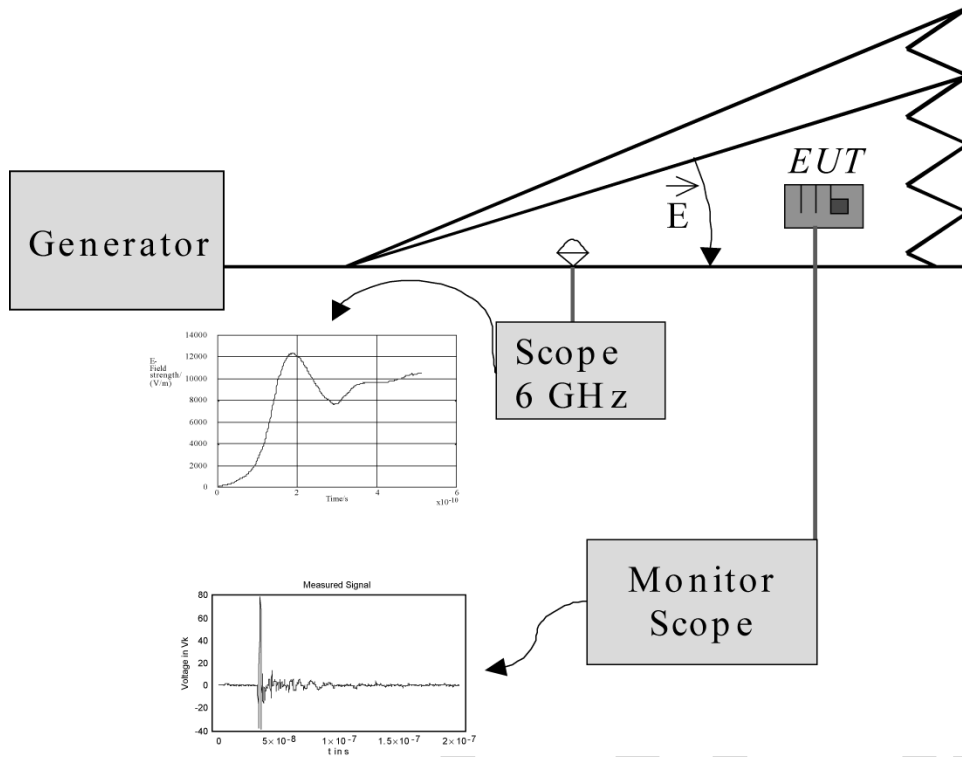


Fig. 4. General measurement setup. <<Author: The font size on graphs is too small in contrast to font size in squares. Is it possible to fix and resubmit for improved viewing?>>

TABLE II  
TESTED TECHNOLOGIES

TTL-Technology					
Standard	Schottky (S)	Low Power Schottky (LS)	Advanced Schottky (AS)	Advanced Low Power Schottky (ALS)	Fairchild Advanced Schottky (FAST)
CMOS-Technology					
High Speed (HC)	High Speed TTL-compatible (HCT)		Advanced (AC)	Advanced TTL-compatible (ACT)	

Fig. 6 shows the BFR and DFR of NAND-devices built in four different CMOS technologies. The comparison of CMOS, with TTL-NAND device shows, that the destruction thresholds are similar, but that TTL-NAND devices only show nonreversible destructions. At lower field amplitudes no breakdowns occurred in the TTL NAND devices in contrary to the behavior of CMOS-NAND devices (see Fig. 7).

Fig. 8 shows the Breakdown (BT) and (DT) of NAND-devices built in ten different technologies (compare Table II). The same effects were observed during the investigation of inverter devices (Fig. 9).

**B. Microcontroller**

Three different types of microcontrollers with a different number of I/O-ports have been investigated. The basic features of the microcontrollers are as follows:

- RISC architecture;

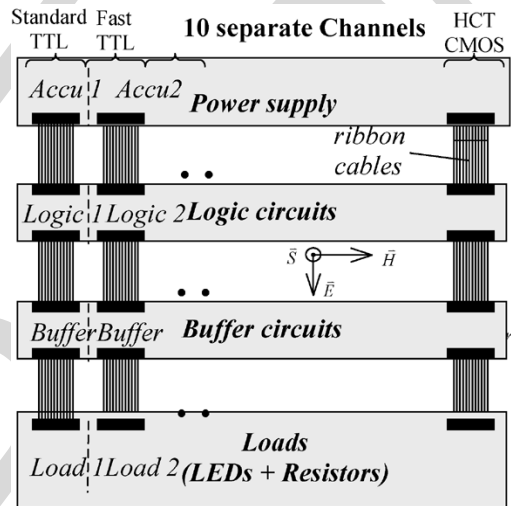


Fig. 5. Test setup: principle.

- high-speed CMOS technology;
- 32 × 8 general purpose working registers;
- flash on board;
- EEPROM on board;
- power supply  $V_{CC}$ .

The influence of different data, reset, osc., <<Author: Please spell out "osc." thank you>> and power supply-line lengths has been tested as well as a variation of the clock rate.

Fig. 10 shows the basic elements of a microcontroller circuit and the modified parameters. Four microcontrollers of the same type have been tested simultaneously to observe any difference. The microcontroller circuits were placed vertically on a wooden

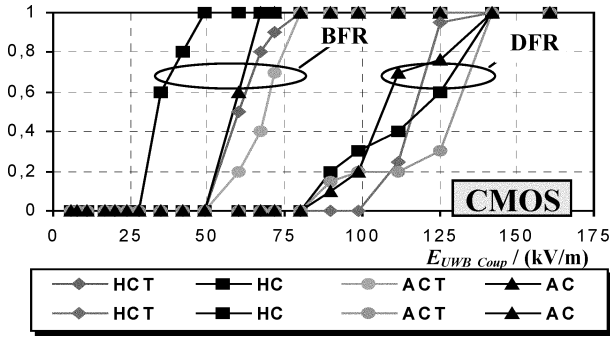


Fig. 6. Breakdown (BFR) and DFR of CMOS NAND devices.

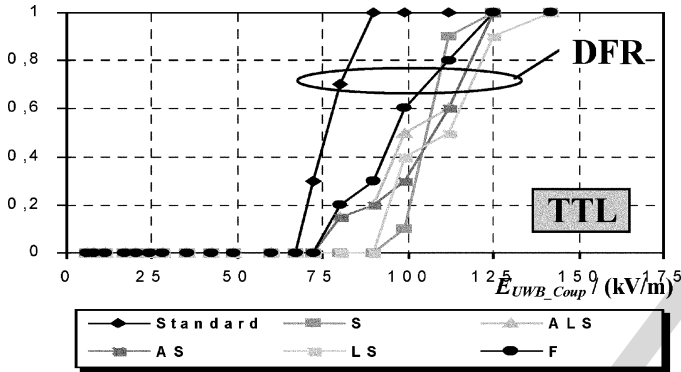


Fig. 7. DFR of TTL NAND devices.

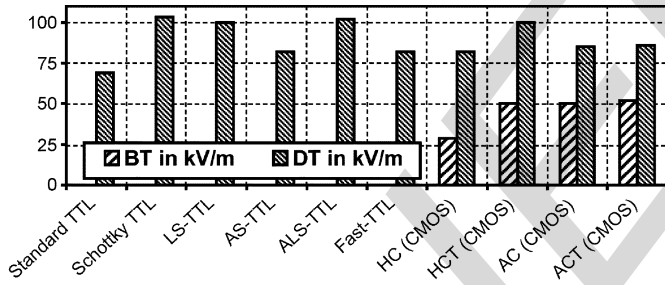


Fig. 8. Breakdown (BT) and DT of CMOS and TTL NAND devices.

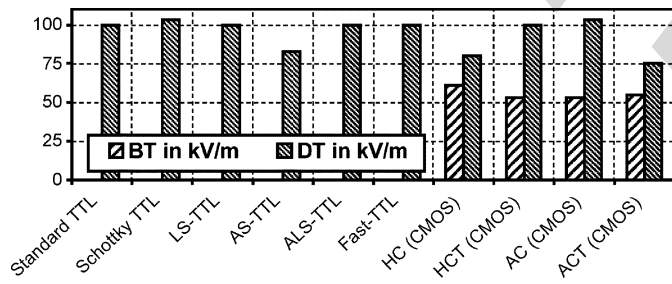


Fig. 9. Breakdown (BT) and DT of CMOS and TTL inverter devices.

wall (see Fig. 11). The different states of the I/O-ports are monitored via different colored LEDs.

The variation of the data-, osc., reset-, and power supply-line length was done with ribbon cables.

During the test, a program was running on the microcontrollers which can get into two different states. In status 1, two ports are high and two ports are low to observe this state. After

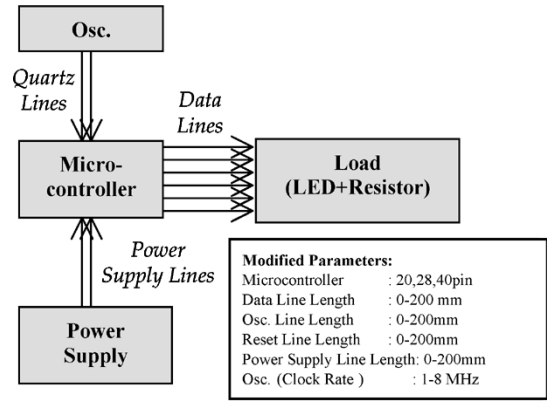


Fig. 10. Basic microcontroller circuit and modified parameters.

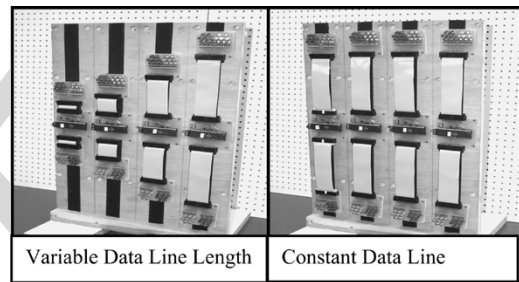


Fig. 11. Microcontroller test setup.

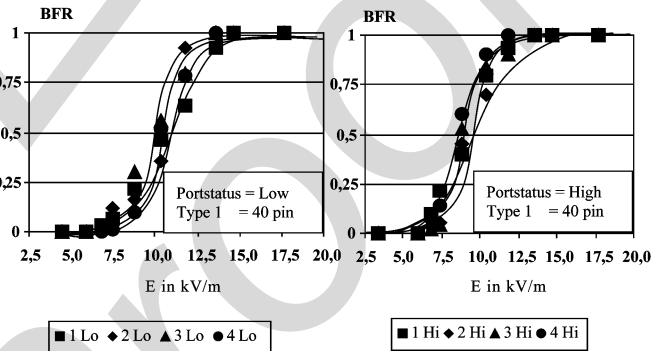


Fig. 12. BFR for microcontroller type 1 (40 pin) at basic setup.

a switch, the program moves to the second state in which the microcontrollers were exposed to the pulses. The intention was to observe a self reset of the system by changing from state 2 back to state 1. Without the implementation of two states a self reset cannot be observed due to the fast reset action. In state 2, the I/O-Ports are changing from low to high to investigate the influence of the port state on the susceptibility. As the basic configuration a state with a minimal osc., reset-, data-, and power supply-lines length and a clock rate of 1 MHz was defined. Figs. 12 and 13 show the results for two different types of microcontrollers in the basic configuration. For the microcontroller circuits, BT and BB do not vary significantly when different devices of the same type of microcontroller were tested as shown in Figs. 12 and 13, but are significantly influenced by the microcontroller type. In the analysis, the breakdown parameters BT and BB have been determined as the average over the BT and BB of four microcontrollers of the same type.

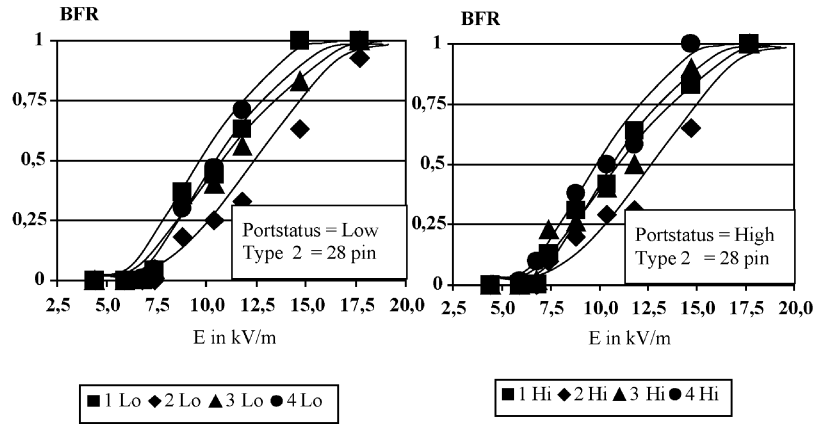


Fig. 13. BFR for microcontroller type 2 (28 pin) in a basic configuration.

TABLE III  
INFLUENCE ON BT AND BB

	Data Line Length	Reset Line Length	Osc. Line Length	Power Supply Line Length	Clock Rate	Type of Controller
<b>BT</b>	Low	High	Medium	Medium	None	Low
<b>BB</b>	None	High	Low	Medium	None	High

The BT of the tested microcontrollers was generally significantly influenced by the reset line length, influenced by the clock- and power supply line length, not much influenced by the data line length and the type of microcontroller and not influenced by the clock rate (up to 8 MHz). These results are shown in Table III.

The BB is generally significantly influenced by the type of microcontroller and the reset line length, influenced by the power supply-line length, not much influenced by the osc. line length, and not influenced by the data line length and clock rate.

### C. Microprocessor Boards

In this section, the results of the determination of the susceptibility levels of microprocessor boards (MB) in several different test facilities are presented. Examined were two different MB as follows:

- 1) SSC 5 × 86 AMD 133 MHz;
- 2) Rocky-518 HV Pentium/MMX 233 MHz.

In Table IV, the important parameters of the applied pulses are listed. To compress the large number of results of all those tests to a manageable number, for HPM and cw signals the highest (HL) medium (ML) and smallest (SL) susceptibility level over the frequency was determined. The HL (ML) is the highest (average) field strength needed to disrupt the EUT over all tested frequencies. Accordingly, SL is the smallest field strength needed to disrupt the EUT over all tested frequencies, this means that the frequency of the SL is the most susceptible frequency of the EUT.

TABLE IV  
PARAMETERS OF THE TEST PULSES

Pulse Shape	Parameter 1	Parameter 2	Parameter 3
EMP 10	$t_r$ 10 ns	$t_{fwhm}$ 200 ns	$E_{max}$ up to 50 kV/m
EMP 1	$t_r$ 1 ns	$t_{fwhm}$ 80 ns	$E_{max}$ up to 50 kV/m
WIS UWB up	$t_r$ 90 ps	$t_{fwhm}$ 2.5 ns	$E_{max}$ up to 30 kV/m
WIS UWB bp	$t_r/t_f$ 100 ps	$t_d$ 350 ps	$E_{max}$ up to 20 kV/m
Rheinmetall UWB bp	$t_r/t_f$ 200 ps	$t_d$ 500 ps	$E_{max}$ up to 40 kV/m
HPM	<i>Freq.-Range</i> 150 MHz –	<i>PRF</i> 1 Hz –	$E_{max}$ up to 4 kV/m
dwll time 1 s	3.4 GHz	1 kHz	
cw	80 MHz –	dwll time	up to 1 kV/m
	1000 MHz	1 s	

For pulsed signals another quantity is of importance: the BB. The lower border of the BB represents a low probability of disruption by a single pulse, so a high PRF (HPRF) <<Author: Please define “PRF” thank you>> is needed to disrupt the MB, the upper border represents a high probability for a disruption by a single pulse, so only a low PRF (LPRF) is needed to disrupt the MB. The compressed results of the susceptibility levels of the MB are shown in Fig. 14 for EMP and UWB pulses and in Fig. 15 for HPM and cw signals. The susceptibility of the 133 MHz MB is comparable to the shown results.

A first look at those susceptibility levels leads to the following results. The difference between the susceptibility levels of long HPM pulses and cw signals is small. The duration of HPM pulses (above a certain minimal duration) has nearly no influence on the susceptibility levels of the MB. The effect of the repetition rate of the HPM pulses on the susceptibility levels of the MB is only of minor significance. The SL value for both MB is about a few 100 V/m, the HL value of both MB is located between 1–2 kV/m. The effect of a rising of the PRF for EMP and UWB pulses is significantly lowering the susceptibility levels. The susceptibility levels are extremely dependent on the pulse shape (in the case of the used pulse shapes the maximal difference of the susceptibility levels was a factor of 25 in necessary field strength). The lowest susceptibility levels for EMP and UWB pulses are a few kilovolt per meter.

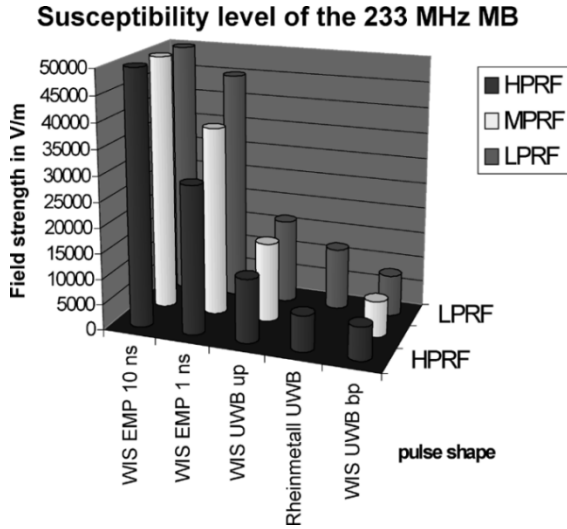


Fig. 14. Susceptibility levels of the 233-MHz MB to EMP and UWB.

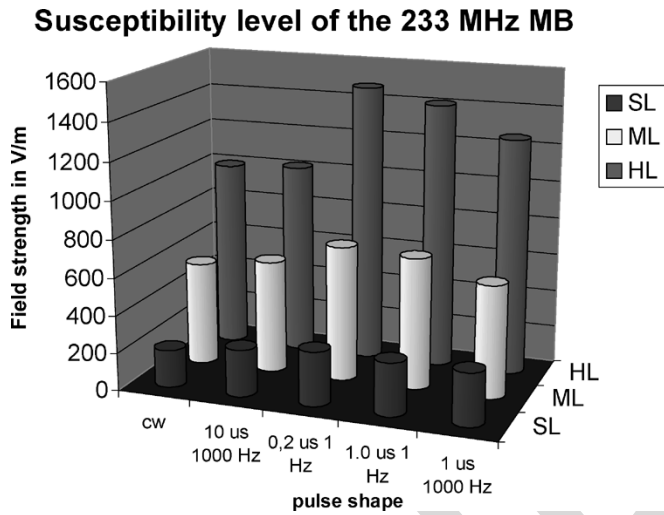


Fig. 15. Susceptibility levels of the 233-MHz MB to HPM and cw signals.

For a more detailed evaluation of the results with regard to the susceptibility levels and the pulse characteristics one has to take some more complex time- and frequency domain quantities into account which have to be determined and discussed. In the following, quantities that were selected for the detailed evaluation are introduced. In the time domain the maximal amplitude  $A(t)$  (HL and SL for HPM and cw signals and HPRF and LPRF for EMP and UWB pulses), the overall energy density of the field signal  $\hat{E}(t)$ , the PRF efficiency and the frequency efficiency

$$\eta_{\text{PRF}} = \frac{E_{\text{HPRF}}}{E_{\text{LPRF}}} \quad \text{and} \quad \eta_{\text{Freq}} = \frac{E_{\text{SL}}}{E_{\text{HL}}}$$

were selected. In the frequency domain the maximal spectral amplitude  $A(f)$ , the average spectral amplitude  $\rho_A$  and energy density  $\rho_E$  and the amplitude- and energy efficiency  $\eta_A$  and  $\eta_E$  were selected in the frequency range from 100 MHz to 3 GHz, because in that frequency range the coupling efficiency of the MB is optimal [6]. One of the most important quantities for the evaluation of HPM pulses is  $\eta_{\text{Freq}}$  because it is a measure for the effectiveness of a HPM pulse in the case that the

system transfer function, the orientation of the system, and the actual layout of the cable bundles of the target system are not known. The frequency efficiency of both MB for the different pulse shapes has an average of about 0.2, which leads to the assumption that the quality of the coupling resonances is very low (near 5). A similarly important quantity is  $\eta_{\text{PRF}}$  for EMP and UWB pulses because it determines whether it makes sense to use repetitive pulses for disrupting a given system or not. The PRF efficiency of the two MB for all used EMP and UWB pulse shapes has an average value of 0.7, which means that the usage of a repetitive system would lower the susceptibility level by approximately 30%, compared to a single-shot system. Although there are other parameters that could be compared, the energy density that is necessary for a disruption of the MB is of large importance for the selection of the source and the power supply, and determines their weight and size. This energy density is shown in Fig. 16 for two cases: best-case (black): the SL value for HPM and cw signals, and the HPRF level for EMP and UWB pulses); and worst-case (gray) the HL value for HPM and cw signals and the LPRF level for EMP and UWB. Depending on the pulse shape, some pulses need a million times the energy other pulses need for a disruption of the MB functionality. Noticeable is that the most effective HPM pulse in the best case scenario (SL) needs only 2 or 3 times the energy a UWB pulse needs to disrupt the MB. In the worst-case scenario, the most effective HPM pulse needs 60–70 times the energy of the UWB pulse.

The large differences in the susceptibility levels for different EMP and UWB pulses are demonstrating that an evaluation of the pulse efficiencies in the time domain is not sufficient. The determination of the energy- and amplitude efficiencies is making clear why those susceptibility levels differ that much. The pulses which do not have distributed their power and energy in the for MB relevant spectral range [2] have a very low energy- and amplitude efficiency which does analytically explain the measured values. Even the highest measured difference for a disruption necessary energy of the different pulses ( $10^6$ ), and the maximal difference of the energy efficiency is the same (factor of  $10^6$  between EMP 10 and WIS UWB bp).

The average spectral amplitudes of the pulses determine the amount of coupled voltage or current in the system. The average spectral amplitude of  $10^{-5}$  V/m/Hz at the for the disruption of the MB necessary field strengths is the same for all pulse shapes. A HPM signal needs between 2 and 71 times the energy a UWB pulse needs to disrupt the MB but only a factor of 0.03 to 0.45 of the field strength.

#### D. PC Systems

During the investigation, the tested PC systems were operated in a minimal configuration which consists of mainboard, processor, random access memory, and accumulator power supply. For monitoring the function of the systems, an ISA-bus monitor card has been developed which allows to monitor data lines, address lines, and internal system states separately. Those systems were placed in the waveguides in such, that coupling into the monitor card is minimal. A simple DOS version has been chosen as the operating system to avoid breakdowns as a result of a higher level operation system. The operation system as well

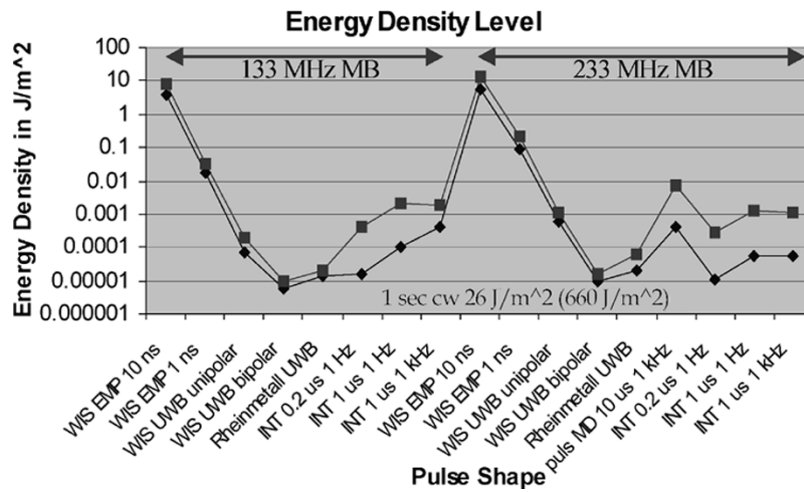


Fig. 16. Energy density of the pulses for both MB.

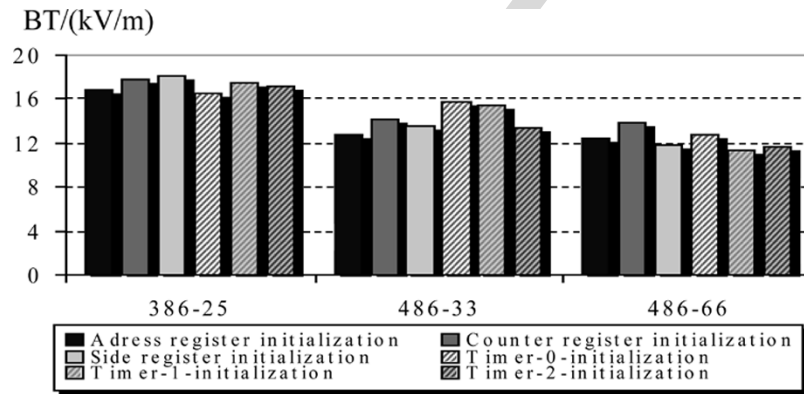


Fig. 17. BT of three PC systems in six different program states.

as the test programs were loaded directly before the test from a floppy disk drive, so that no hard disk drive was necessary.

To observe the influence of different program states concerning the susceptibility of personal computers, a test program with separate subroutines has been implemented in the investigated PC systems. Different hardware elements [direct memory access (DMA) controller and programmable interval timer (PIT) module] on the mainboards were activated. The DMA-main-routine as well as the PIT-main-routine is separated into three subroutines with different functions inside the DMA-controller resp. the PIT-module. During each subroutine, the pulses have been applied to the systems. After each subroutine, a CPU test has been performed to make sure that the complete system was working properly. Fig. 17 shows the breakdown thresholds BT of three personal computer systems for an UWB testpulse with a rise time of  $t_r = 100 \text{ ps}$  and a pulse length of  $t_{fwhm} = 2.5 \text{ ns}$ .

Neither in the main routines nor in the sub routines a significant change of the breakdown thresholds BT has been observed. The BT gets smaller the higher the generation of the technology is. Similar results have been observed if pulses with other rise times and pulse lengths were applied.

### E. PC Networks

The susceptibility levels of a PC network consisting of two i486 based personal computers and an Ethernet connection to unipolar UWB pulses with a rise time of 100 ps, a full width half max time of 2.5 ns and an amplitude of 100 V/m to 12 000 V/m was tested. Several network configurations and cables were used:

- 10Base2;
- 10BaseT;
- 100BaseTX;
- Ethernet Hub;
- RG 58 RG 223, S-UTP and S-STP cables;
- 10 and 100 Mb;

To eliminate the susceptibility effects of the PCs we shielded the two PCs with movable absorber walls (see Fig. 18).

The data line was exposed to the UWB pulses and the number of bit errors, lost data frames, and PC breakdowns was monitored. A collision between signal bits on the network and a coupled UWB pulse is shown in Fig. 19. The coupled pulse resulted from a 12 kV/m UWB pulse coupling into a RG 58 cable. The amplitude of the coupled pulse was 90 V.

The UWB field strength level which leads to bit errors, lost frames, or to a breakdown of the network are shown in Fig. 20. Bit errors occur when the amplitude of the coupled pulse is comparable to the voltage level of the bits. Data frames are lost when

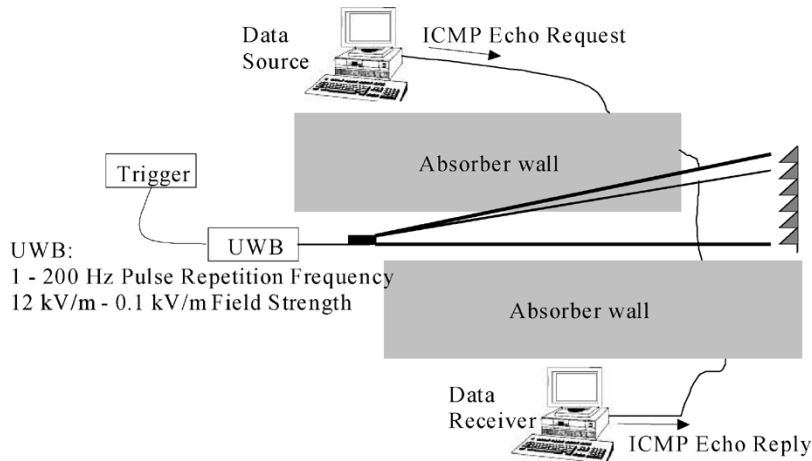


Fig. 18. Measurement setup for the PC network tests.

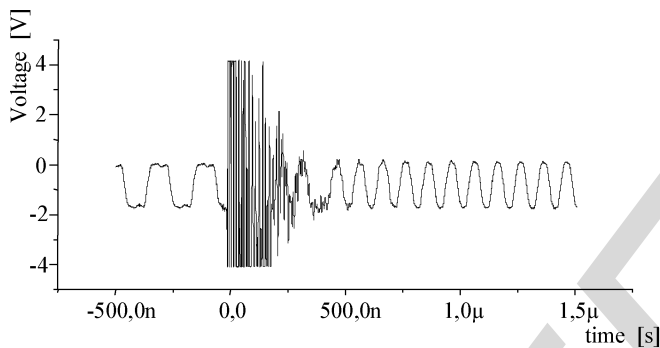


Fig. 19. Collision of a coupled UWB pulse with data bits.

a substantial part of the frame is destroyed by the coupled pulse. This quantity rises linearly with the pulse repetition frequency. A breakdown occurs when the coupled signal is so large, that the network hardware locks or resets.

The susceptibility depends strongly on the shielding effectiveness of the used cables and the technology used (see Fig. 23 <<Author: There was no submission for a Fig. 23, please submit a Fig. 23, or change sentence with reference to Fig. 23 accordingly, thank you>>). The lowest UWB field strength level for bit errors is 200 V/m, for lost frames about 4 kV/m and for breakdowns about 6 kV/m [6].

#### F. Microscopic Analysis of Destruction Effects

The microscopic analysis of the destructed devices generally shows three different damaging levels (Fig. 21). At lower field strengths (level 1) only electronic components like diodes or transistors on the chip were damaged, mostly as a result of flashover effects (Fig. 21). If the amplitude of the electromagnetic pulse increases by about 50%, additional on chip wire destructions (this means smelting of pcb tracks without flashover effects) and multiple component destructions occurred (Fig. 21, level 2). Further increase of the amplitude leads to additional bond wire destructions (Fig. 21), multiple component, and on chip wire destructions (level 3).

Fig. 22 shows the DFR of TTL-inverter devices, separated to component, on chip wire, and bond wire destructions. At the lowest field level component destructions occurred. A further

### Susceptibility Level of PC Networks

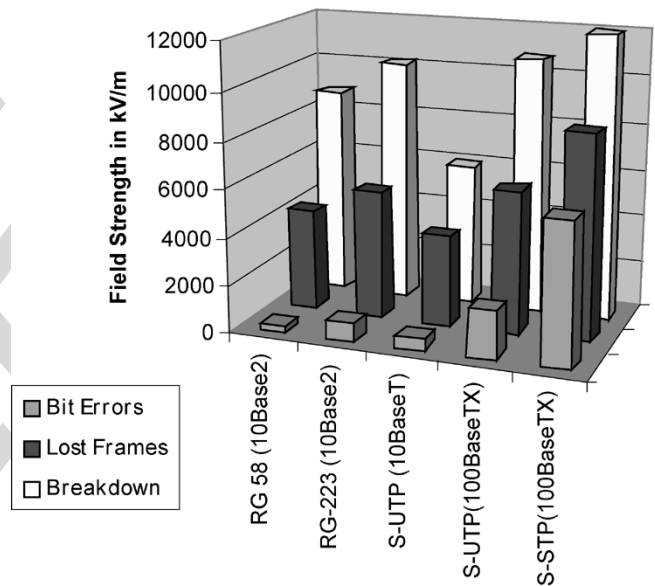


Fig. 20. Susceptibility level of PC networks.

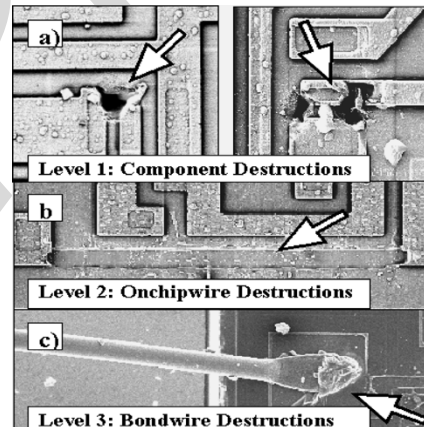


Fig. 21. Destruction effects on chip level.

rising of the field strength resulted in on chip wire and bond wire destructions. The components on the chip, which were damaged



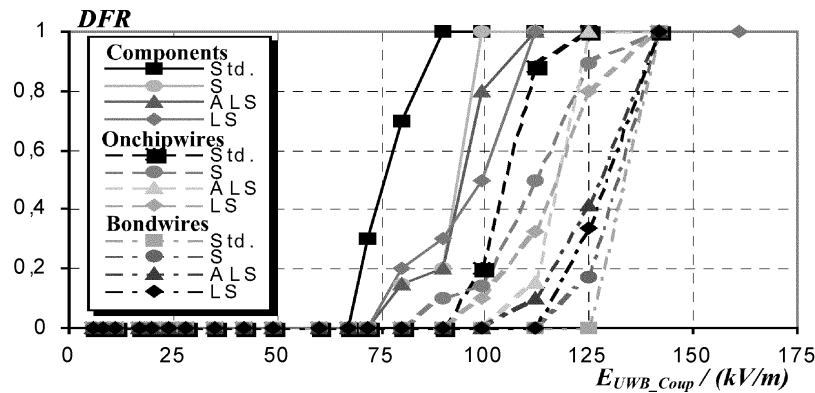


Fig. 22. DFR of TTL NAND devices separated into component bond wire and on chip wire destructions.

TABLE V  
SUSCEPTIBILITY LEVELS BT (DT)

EUT	UWB in kV/m	EMP in kV/m	HPM in kV/m
Logic Devices	25 (75)	120	
Microcontroller	7.5	42	
Microprocessor Boards	4	25	0.2
PC Systems	12		
PC Networks	0.2	0.5	

first if the amplitude of the electromagnetic pulse was increased, are depending on the layout of the chip (and therefore on the manufacturer) as well as on the technology.

Transistors, diodes, and resistors were damaged similarly. The reproducibility of the destruction effects on chip level in the used measurement setup is very high. On that account it is possible to predict the destruction effects of integrated circuits on chip level, if the proposed measurement setup is used.

## VI. CONCLUSION

The main goal of this paper was to give a brief overview of the susceptibility levels of modern electronic equipment as well as the breakdown and destruction effects. In Table V, the susceptibility levels (lowest observed field strength for a disruption of the functionality of the EUT) of all tested devices are shown. Generally the level is lower the more complex the device under test is. The investigation of the destruction effects show, that even UWB pulses have sufficient energy to destroy on chip structures.

## REFERENCES

- [1] D. Nitsch, F. Sabath, C. Mojert, M. Camp, and J. L. ter Haseborg, "Susceptibility of electronic equipment to transient electromagnetic fields of various waveforms," in *Proc. Int. Conf. Electromagnetics in Advanced Applications, ICEAA*, Turin, Italy, Sept. 2001, pp. 213–216.
- [2] D. Nitsch and F. Sabath, "Prediction of ultra wide band coupling to modern electronic equipment," in *Proc. EMC Wroclaw*, Wroclaw, Poland, June 2002, pp. 103–108.

- [3] <<Author: Please provide page numbers, thank you>>D. Nitsch, J. Schlüter, and H. J. Kitschke, "Generierung und vorteile von ultrawideband-impulsen," in *Proc. EMV99*, Mannheim, Germany, 1999.
- [4] <<Author: Please identify "type" of reference and provide city/state/month/year/page numbers, if necessary, thank you>>C. Braun, Aufbau eines breitbandigen Wellenleiters für NEMP Modell Simulationen.
- [5] <<Author: Please provide publisher city/state information, thank you>>E. Haselhoff, *Latchup, ESD, and Other Phenomena*. Dallas, TX: Texas Instruments, 2000.
- [6] <<Author: Please provide page numbers for reference, thank you>>C. Mojert, D. Nitsch, H. Friedhoff, J. Maack, and M. Camp, "UWB and EMP susceptibility of modern computer networks," in *Proc. EMC Zürich 2001*, Zurich, Switzerland, Feb. 2001.



**Daniel Nitsch** (A'98–SM'00) was born in Euskirchen, Germany, in 1969. He received the Dipl.-Phys. degree from the University of Hamburg, Hamburg, Germany, in 1994.

In 1994, he joined the Federal Office of Defense Technology and Procurement (BWB). Currently, he is Branch Head of the Electromagnetic Effects Branch at the Federal Armed Forces Scientific Institute for Protective Technologies and NBC-Protection (WIS), Munster, Germany. His research interests include investigations of susceptibility of electronic systems and components, wide-band and ultra-wide-band coupling to complex systems and pulse forming networks. He is the author or coauthor of more than 50 scientific papers



**Michael Camp** (S'XX) <<Author: Please provide membership year information, thank you>> received the Dipl.-Ing. degree in electrical engineering from the University of Hanover, Hanover, Germany, in 1999, and is currently pursuing the Ph.D. degree at the Institute for Electrical Engineering and Measurement Science at the same university.

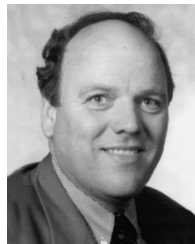
His research interests include high-frequency measurement techniques and the susceptibility of electronics to fast transient pulses (UWB). He is the author or coauthor of more than 20 scientific papers.



**Frank Sabath** (M'94) was born in Werther, Germany, in 1966. He received the Dipl.-Ing. degree in electrical engineering from the University of Paderborn, Paderborn, Germany, in 1993, and the Dr.-Ing. degree from the University of Hannover, Hannover, Germany, in 1998.

From 1993 to 1998, he was with the C-Lab, a Joint Research and Development Institute of the University of Paderborn and the Siemens Nixdorf Informationssysteme AG, Paderborn, Germany, where his responsibilities included research activities on numerical field calculation and the radiation analysis of printed circuit boards. Since 1998, he has been with the Federal Office of Defense Technology and Procurement (BWB). Currently, he is a Scientist with the Federal Armed Forces Scientific Institute for Protective Technologies and NBC-Protection (WIS), Munster, Germany. His research interests include investigations of electromagnetic field theory, numerical field computation, investigations of short pulse interaction on electronics, and impulse radiation.

Dr. Sabath is a Member of URSI Com. E. <<Author: Please spell out "URSI Com. E." thank you>>



**Heyno Garbe** (SM'XX) <<Author: Please provide membership year information, thank you>> was born in Germany in 1955. He received the Dipl.-Ing. and Dr.-Ing. degrees from the University of the Federal Armed Forces, Hamburg, Germany, in 1978 and 1986, respectively.

Since 1992, he has been with the University of Hannover, Hannover, Germany, where he is currently a Professor in the Department of Electrical Engineering and Information Technology. From 1986 to 1991, he was with the Asea Brown Boveri

Research Center, Baden, Switzerland. From 1991 to 1992, he was the Research Manager for EMC Baden Ltd.

Prof. Garbe is the convener of the Joint Task Force CISPR/A and TC77B on TEM Waveguides and is very active in several EMC-related national and international standardization committees. He is an Associate Editor of the IEEE TRANSACTIONS ON ELECTROMAGNETIC COMPATIBILITY and a Counselor for the IEEE Student Branch. He is a Member of URSI Com. E, VDE <<Author: Please define "URSI Com. E, VDE" thank you>>.



**Jan-Luiken ter Haseborg** (M'87-SM'94-F'00) received the Dipl.-Ing. degree from the Technical University of Braunschweig, Braunschweig, Germany, in 1974, and the Dr.-Ing. degree from the Rheinisch Westfälische Technische Hochschule (RWTH), Aachen, Germany, in 1978.

From 1975 to 1983, he was a Scientific Assistant and Senior Scientist at the Federal Armed Forces University, Hamburg (UniBwH), Germany. Since 1984, he has been a Professor of Electrical Engineering and EMC at the Technical University

Hamburg-Harburg (TUHH), Germany, and since 1990 he has been Head of the Department of Measurement Engineering and EMC of TUHH. He is the author and coauthor of more than 50 scientific papers

Dr. ter Haseborg received an Honorary Doctorate from the University of Rostock, Rostock, Germany, in 2002. He is an Associate Editor of the IEEE TRANSACTIONS ON ELECTROMAGNETIC COMPATIBILITY. In 1998, he was elected an EMP Fellow (Summa Foundation, USA). He is also a Member of the "Schutzkommission" of the BMI (Department of the Interior, Germany).